

0017-9310(94)00327-0

The flows induced by a heated oscillating sphere

D. V. LYUBIMOV,† A. A. CHEREPANOY,† T. P. LYUBIMOVA‡ and B. ROUX§

†Theoretical Physics Department, Perm State University 15, Bukirev Street, 614600, Perm, Russia

‡Institute of Continuous Media Mechanics, RAS 1, Korolyov Street, 614061, Perm, Russia

§Institut de Mecanique des Fluides 1, Rue Honnorat, 13003, Marseille, France

(Received 12 September 1994)

Abstract—Time-averaged flows induced by oscillations of a heated (or cooled) solid sphere immersed in a liquid are investigated. The cases of an infinite surrounding liquid and the liquid placed into the spherical rigid envelope are considered. The gravity is absent. The interaction of thermovibrational flows and vibrational Schlichting flows is studied. New generalized equations are used for the description of thermovibrational convection. Analytical solutions have been obtained for small values of the governing parameters, under restriction of creeping flows, both in the case of infinite surrounding liquid and liquid placed into the rigid envelope. It has been found that the vibrational flow essentially depends on the layer thickness and can be rather complicated in the case of small thicknesses. At a fixed layer thickness, the creeping flow structure is defined by only one parameter, which is the ratio of vibrational Grashof number and Schlichting parameter. In the case of arbitrary values of the parameters, vibrational flows have been studied by a finite-difference method. The evolution of the finite-amplitude vibrational flow structure with the increase of the vibrational Grashof number has been investigated.

1. INTRODUCTION

It is known that the high frequency vibrations of the body immersed in a liquid induce time-averaged flow in that liquid. Different mechanisms of flow generation can occur. One of them, found by Schlichting [1], acts even in uniform fluid (of constant density). In this case the pulsating flow in the thin viscous skin-layer near the vibrating body surface is of vortical nature and, due to non-linear interaction, leads to time-averaged flow which is a vortex one as well. If the fluid density is non-uniform, for example due to non-isothermality, the additional mechanism for the time-averaged flow generation is at work. Flows of this type have been studied before [2]. In most works the particular case of a fluid completely filling the vessel subject to progressive vibrations is investigated. The equations for the time-averaged flow of that origin, called thermovibrational convection, have been obtained in ref. [3] by averaging the convection equation in the Boussinesq approximation. The recent analysis of Lyubimov [4] has demonstrated that the approach developed in ref. [3] becomes invalid in the case when the vibrations are non-uniform, as for example in the case when only some part of the body immersed in a liquid vibrates, while the others are at rest. Thermovibrational time-averaged flow exists in this case as well, but this flow has to be described by different equations, namely the ones obtained in ref. [4].

In this paper we study the interaction of different mechanisms for time-averaged flow generation in the

case of a simple geometry. The flow is induced by the vibrations of a solid sphere immersed in a fluid contained in a fixed spherical envelope so that the time-averaged position of the internal sphere coincides with the center of the envelope. The temperatures of the internal sphere and envelope are different, so the fluid completely filling the space between the spheres is non-isothermal. To exclude the effect of the usual gravitational convection we consider the case of a zero gravity.

2. GOVERNING EQUATIONS—BOUNDARY CONDITIONS

Let us consider the case when the internal sphere vibrates along the axes given by unit vector \mathbf{k} according to sinusoidal law with the amplitude a and the frequency ω . We study the high frequency vibrations of small amplitude so that the conditions

$$\omega \gg \nu/L^2 \quad (1)$$

and

$$a \ll L \quad (2)$$

are satisfied. Here ν is the kinematic viscosity, L is the characteristic size. We assume that the inequality (2) is satisfied at $L = \min(r_1, r_2, r_2 - r_1)$, where r_1 is the radius of the internal sphere. As shown in ref. [4], if the conditions (1)–(2) are satisfied, then the time-averaged flow is described by the following equations:

slip one because the system (6)–(8) describes the field of the pulsating velocity correctly everywhere except in the viscous skin-layers near the rigid surfaces, but the thickness of skin-layers are rather small due to relation (1).

The thermal conductivities of solid bodies are assumed to be high, so that we can impose the isothermality conditions on that surfaces:

$$T = 0 \quad \text{at} \quad r = R \quad (9)$$

and

$$T = 1 \quad \text{at} \quad r = 1 \quad (10)$$

the envelope temperature being chosen as the reference one.

The pulsating part of velocity is not potential in the viscous skin-layers near the solid body surfaces. It is of vortical nature. This leads to the generation of the time-average vortex flow which can be described by specific boundary condition for the average velocity [1, 5]. In our case this boundary condition is

$$\mathbf{v}_\tau = -Sc \left[\frac{1}{2} \nabla_\tau \mathbf{U}_\tau^2 + 2 \mathbf{U}_\tau \cdot (\nabla_\tau \mathbf{U}_\tau) \right] \quad (11)$$

on the surface of the envelope, at $r = R$, and

$$\mathbf{v}_\tau = -Sc \left[\frac{1}{2} \nabla_\tau \mathbf{W}_\tau^2 + 2 \mathbf{W}_\tau \cdot (\nabla_\tau \mathbf{W}_\tau) \right] \quad (12)$$

on the vibrating sphere surface, at $r = 1$.

Here $\mathbf{U} = \nabla \Phi$, and $\mathbf{W} = \mathbf{U} - \mathbf{k}$ is the amplitude of the pulsating velocity in the reference frame connected with the vibrating sphere. The subscript τ stands for the tangential components of vectors; operator ∇_τ acts along the solid bodies surfaces. Strictly speaking, the conditions (11)–(12) are satisfied on the external borders of the viscous skin-layers, but due to the small values of their thickness, relation (1), we can impose the conditions (11)–(12) on the solid body surfaces.

Boundary conditions (11)–(12) include one more non-dimensional parameter, $Sc = a^2 \omega / \nu$, which is responsible for the time-averaged vortex flows generation in the skin-layers.

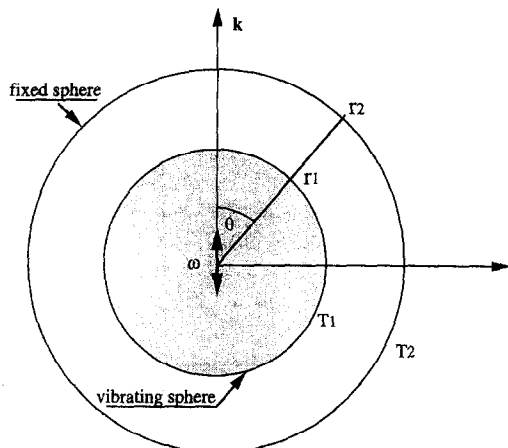


Fig. 1. Schematic description of the problem and coordinates definition.

We restrict ourselves with the axisymmetrical solutions, i.e. we assume that the non-zero tangential components are only θ -components. Then, the conditions (11)–(12) take the form:

$$v_\theta = -Sc \left\{ 3 \frac{\partial \Phi}{\partial \theta} \frac{\partial^2 \Phi}{\partial \theta^2} + 2 \cot \theta g \theta \left[\frac{\partial \Phi}{\partial \theta} \right]^2 \right\} \quad \text{at} \quad r = R \quad (13)$$

and

$$v_\theta = -Sc \left\{ 3 \frac{\partial \Phi_1}{\partial \theta} \frac{\partial^2 \Phi_1}{\partial \theta^2} + 2 \cot \theta g \theta \left[\frac{\partial \Phi_1}{\partial \theta} \right]^2 \right\} \quad \text{at} \quad r = 1 \quad (14)$$

where $\Phi_1 = \Phi \cos \theta$.

The normal components of the time-averaged velocities satisfy the impermeability condition:

$$v_r = 0 \quad \text{at} \quad r = 1 \quad \text{and at} \quad r = R. \quad (15)$$

The problem (6)–(8) has the solution:

$$\Phi = \frac{\cos \theta}{1 - R^3} \left[\frac{R^3}{2r^2} + r \right]. \quad (16)$$

By substituting equation (16) into equations (3) and (13) we obtain the closed problem for the time-averaged velocity \mathbf{v} and temperature T . In axisymmetrical case it is convenient to introduce the streamfunction Ψ :

$$v_r = \frac{1}{r \sin \theta} \frac{\partial(\Psi \sin \theta)}{\partial \theta} \quad (17)$$

$$v_\theta = \frac{1}{r} \frac{\partial(r\Psi)}{\partial r}. \quad (18)$$

For the solution (17)–(18), equation (4) is satisfied identically and equations (3) and (5), with the boundary conditions (13)–(14) for stationary flows, take the form:

$$M(\Psi, \zeta) + \frac{Gv}{r} \left[\frac{\partial E}{\partial r} \frac{\partial T}{\partial \theta} - \frac{\partial E}{\partial \theta} \frac{\partial T}{\partial r} \right] = L\zeta \quad (19)$$

$$\zeta = -L\Psi \quad (20)$$

$$M(\Psi, T) = \frac{1}{Pr} \Delta T \quad (21)$$

$$\Psi = 0, \quad \frac{\partial \Psi}{\partial r} = -\frac{45}{8} \frac{Sc}{R(1-R^3)^2} \sin 2\theta \quad \text{at} \quad r = R \quad (22)$$

$$\Psi = 0, \quad \frac{\partial \Psi}{\partial r} = -\frac{45}{8} \frac{Sc R^6}{(1-R^3)^2} \sin 2\theta \quad \text{at} \quad r = 1. \quad (23)$$

The operators M and L are:

$$M(a, b) = \frac{1}{r \sin \theta} \left[\frac{\partial(a \sin \theta)}{\partial \theta} \frac{\partial b}{\partial r} - \frac{1}{r} \frac{\partial(ar)}{\partial r} \frac{\partial b}{\partial \theta} \right]$$

$$L = \Delta - \frac{1}{r^2 \sin^2 \theta};$$

$$\text{with } \Delta = \frac{1}{r^2} \frac{\partial}{\partial r} \left[r^2 \frac{\partial}{\partial r} \right] + \frac{1}{r^2 \sin \theta} \frac{\partial}{\partial \theta} \left[\sin \theta \frac{\partial}{\partial \theta} \right]. \quad (24)$$

The new variable E is proportional to the time-averaged density of the pulsating flow energy:

$$E = \left[\frac{\partial \Phi}{\partial r} \right]^2 + \frac{1}{r^2} \left[\frac{\partial \Phi}{\partial \theta} \right]^2. \quad (25)$$

3. CREEPING FLOWS

At small values of the parameters Gv and Sc it is possible to neglect by non-linear terms in fluid motion and heat transfer equations. Then we arrive at the equations:

$$\frac{Gv}{r} \left[\frac{\partial E}{\partial r} \frac{\partial T}{\partial \theta} - \frac{\partial E}{\partial \theta} \frac{\partial T}{\partial r} \right] = L\zeta \quad (26)$$

$$\zeta = -L\Psi \quad (27)$$

$$\Delta T = 0. \quad (28)$$

The solution of the equation (28) with the boundary conditions (9)–(10) is:

$$T = \frac{R-r}{R-1}. \quad (29)$$

For slow creeping we obtain by substituting equations (16) and (29) into equation (26):

$$L\zeta = -\frac{3R^4 Gv}{4(R-1)(1-R^3)^2} \frac{R^3 - 4r^3}{r^9} \sin 2\theta. \quad (30)$$

It follows from equation (30) and equations (22)–(23) that the solution for Ψ is proportional to $\sin 2\theta$, and by introducing the new variable ψ

$$\Psi = \frac{45R^6}{8(1-R^3)^2} \psi Sc \sin 2\theta$$

one gets from equations (30) and (27):

$$N\zeta = -B \frac{R^3 - 4r^3}{r^9}, \quad (31)$$

$$\zeta = -N\psi, \quad (32)$$

where

$$N = \frac{d^2}{dr^2} + \frac{2}{r} \frac{d}{dr} - \frac{6}{r^2} \quad (33)$$

with the boundary conditions

$$\psi = 0 \quad \frac{d\psi}{dr} = -\frac{1}{R^7} \quad \text{at } r = R \quad (34)$$

$$\psi = 0 \quad \frac{d\psi}{dr} = -1 \quad \text{at } r = 1 \quad (35)$$

where

$$B = \frac{2}{15R^2(R-1)} \frac{Gv}{Sc}. \quad (36)$$

Thus, in the case of weak linear convection, the structure is defined not by two parameters Gv and Sc separately, but by only one parameter, which is the ratio Gv/Sc .

(a) *Limiting case*: $R \rightarrow \infty$

Before studying the convection in a container with the arbitrary ratio of radii R , let us investigate the more simple case when the sphere vibrates in the infinite fluid, i.e. the ratio R tends to infinity. In this case equations (31)–(32) take the form:

$$N\zeta = -\frac{b}{r^9} \quad \zeta = -N\psi \quad (37)$$

and

$$\psi = 0 \quad \frac{d\psi}{dr} = -1 \quad \text{at } r = 1 \quad (38)$$

$$\psi = 0 \quad \frac{d\psi}{dr} = 0 \quad \text{at } r = \rightarrow \infty \quad (39)$$

where

$$b = \frac{2}{15} \frac{Gv}{Sc}.$$

The solution of the problem (37)–(39) is

$$\psi = \frac{1}{r} \left[\frac{b}{504} (r^{-2} - 1)^2 + \frac{1}{2} (r^{-2} - 1) \right] \quad (40)$$

or by returning to the streamfunction Ψ :

$$\Psi = \frac{3}{16r} \left[\frac{Gv}{126} (r^{-2} - 1)^2 + 15Sc(r^{-2} - 1) \right] \sin 2\theta. \quad (41)$$

It follows from equation (41) that, due to the linearity of the equations, the resulting creeping flow is the simple superposition of thermovibrational and Schlichting flows and that this flow is symmetrical with respect to the equatorial plane.

The Schlichting number Sc is always positive. Thus the flow described by the second term in equation (41) is of the same structure at any Sc ; it is the jet flow going away from the sphere pole, and in the equatorial plane the flow is directed towards the body.

The sign of Gv can be different. If the value of Gv is negative, i.e. in the case when the vibrating sphere is colder than the surrounding liquid, the fluid flows induced by thermovibrational and the Schlichting mechanisms are of the same direction. This means that the structure of the resulting flow is the same as that of a pure Schlichting flow. In this case the streamlines are not closed, the liquid particles move from the pole to the infinity, and (near the equatorial plane) from the infinity to the sphere.

The situation is different when the vibrating sphere is warmer than the surrounding liquid. In that case

the fluid flows induced by the two mechanisms are of different direction. Near the vibrating sphere surface the circulation of the flow is defined by the boundary condition (38) and hence the flow here is always directed from equator to the pole. At arbitrary distance from the vibrating sphere the direction of the flow is defined by the competition of the two mechanisms. If the Gv is positive and small enough, then the last term in equation (40) is the main one and the direction of the circulation is the same as in the case discussed above but some of the streamlines become closed. If Gv is higher than the critical value, the flow structure is the 'two-floor' one. There is a separating spherical surface of radius r_* , such as inside the layer limited by that surface the streamlines are closed and the liquid particles do not penetrate outside. The flow direction at $r < r_*$ is defined by equation (38). Outside this spherical layer the streamlines are not closed and the flow direction is of opposite direction (the liquid particles move to the sphere in the polar plane, and from the sphere in equatorial plane). Since at $r = r_*$ the value of ψ should be equal to zero, then we obtain from equation (41)

$$r_*^2 = \frac{b}{b - 252}. \tag{42}$$

It follows from equation (42) that the 'two-floor' structure is possible if b is positive and larger than the critical value equal to 252. In terms of non-dimensional parameters Gv and Sc , the existence condition of the two-floor structure is:

$$\frac{Gv}{Sc} > 1890. \tag{43}$$

The separating spherical surface appears at the infinity at this critical value of the ratio Gv/Sc , and moves to the sphere when this ratio increases.

Note that the parameter

$$b = \frac{2}{15\nu} \beta \Theta \omega r_1^2$$

does not depend on the vibration amplitude.

(b) *General case: finite R*

At the finite radius of the envelope, the one-floor flow is impossible since the flows have the same direction near both rigid surfaces, due to the boundary conditions (34) and (35).

The analytical solution of the problem at arbitrary values of R has also been found, but we do not give it here because of the too complicated form.

The streamfunction Ψ defined above has a simple sense: it is the azimuthal component of the vector potential of velocity. However for presentation of the results this function is not the best because the surfaces of constant value of this function (except of the surface $\Psi = 0$) are not the integral surfaces for the velocity field. The needed property belongs to the streamfunction $\hat{\Psi} = \Psi r \sin \theta$. We use for presentation of the

results the radial part of the streamfunction $\hat{\Psi}$, which is defined as $r\psi(r)$.

The results of tabulation for the obtained solutions are presented in Figs. 2–5 for different values of the envelope radius R and of the ratio $k = Gv/Sc$. Here, the vertical axis corresponds to the product $r\psi(r)$, while the horizontal axis corresponds to the relative radial coordinate $y = (r - 1/R - 1)$, with $y = 0$ at the surface of the inner (vibrating) sphere, and $y = 1$ at the surface of the envelope.

As one can see, when the distance between the spheres is large enough (Fig. 2, $R = 4$), the flow structure is similar to that obtained for infinite surrounding liquid. If the temperature difference between the spheres is not too high (curve 1, $k = 2000$), then the resulting flow structure is defined by Schlichting mechanism. The only vortex occupies the space between the spheres, besides, the direction of its circulation corresponds to the Schlichting flow induced in viscous skin-layer near the inner sphere. It is evident that, due to the boundary condition (34), there is the vortex of the opposite direction near the fixed sphere but the intensity of this vortex is so small and it occupies a layer of such small thickness that it is impossible to see it in the graph described under a unique scale. This vortex exists at any value of the parameters but we will not discuss it hereafter because its role is not important due to its small size and intensity.

With the growth of the vibrational Grashof number the influence of thermovibrational flow increases and a vortex of different direction appears (curve 2, $k = 3000$). With further growth of Gv the intensity of thermovibrational flow increases while the intensity of Schlichting flow becomes lower, occupying the smaller area near the inner sphere (curves 3 and 4; $k = 4000$ and 5000). The presence of the envelope results in the larger critical parameters for the appearance of the two-floor structure than that in the infinite surrounding liquid case.

The decrease of the envelope radius leads to the growth of the critical parameters for the transition from one-vortex structure to multi-vortex one (Fig. 3, $R = 2.5$). The structure of the flow becomes more complicated. At the comparatively low values of Gv (Fig. 3, curve 1, $k = 6000$) a one-vortex flow takes place. At higher temperatures of inner sphere the main one-vortex flow remains, but two weak vortices of the same direction develop (curve 2, $k = 8333$). When k exceeds its critical value, the vortex of the opposite direction appears in the central part of the spherical layer (curve 3, $k = 10000$); with the growth of Gv its intensity and size become larger, while the outer vortices replace the inner sphere and envelope (curves 4 and 5; $k = 12000$ and 15000).

Figure 4 corresponds to $R = 2.1$. In this case the influence of Schlichting flow is very large and up to high values of k (curve 1, $k = 50000$) it determines the structure of resulting flow. Only at very high k do the vortices of different direction appear (curves 2, 3, 4; $k = 80000, 100000, 150000$). Note that, in the case

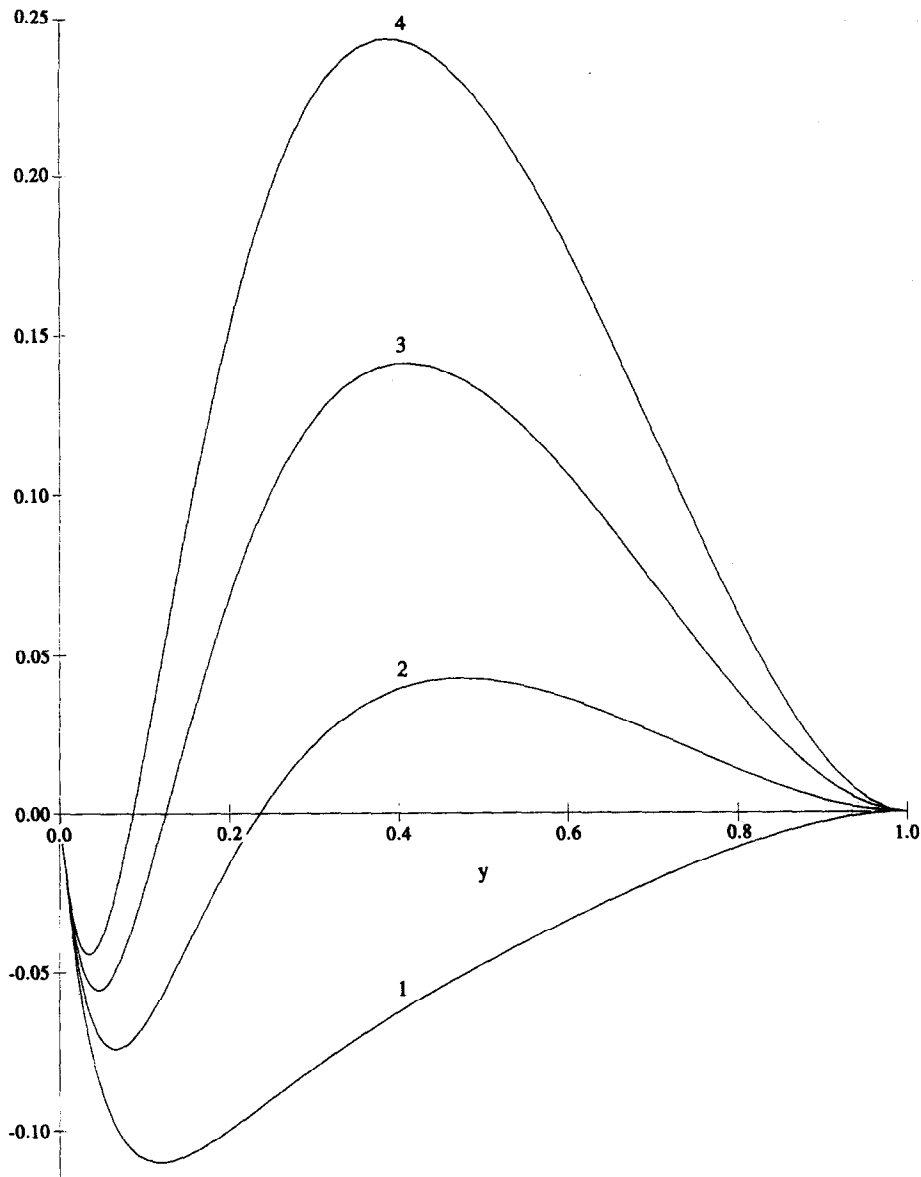


Fig. 2. Radial part of the streamfunction $\Psi/\sin 2\theta$ vs relative radial coordinate $y = (r-1)/(R-1)$ at $R = 4$:
 (1) $k = 2000$, (2) $k = 3000$, (3) $k = 4000$, (4) $k = 5000$.

of such thickness of the layer, the pure thermovibrational flow is of two-vortices structure, the corresponding part of the streamfunction is equal to zero near the point where all the lines cross.

If the inner sphere is cooled (Gv and k are negative) and the layer thickness is large, the flow structure does not change qualitatively with the change of inner sphere temperature. The structure is rather simple, this is one-vortex flow in the direction which corresponds to the Schlichting flow. At smaller values of

the layer thickness the complicated flow structure can exist for the cooled vibrating body (Fig. 5, $R = 2.1$) due to the complicated structure of pure thermovibrational flow. With the increase of absolute value of k , the resulting flow of one-vortex structure (curve 1; $k = -6000$) changes to the two-vortex one (curves 2-5; $k = -10\,000, -15\,000, -20\,000, -25\,000$).

The results discussed above are obtained for the creeping flows which are realized at small values of the parameters Gv and Sc . To study the non-linear

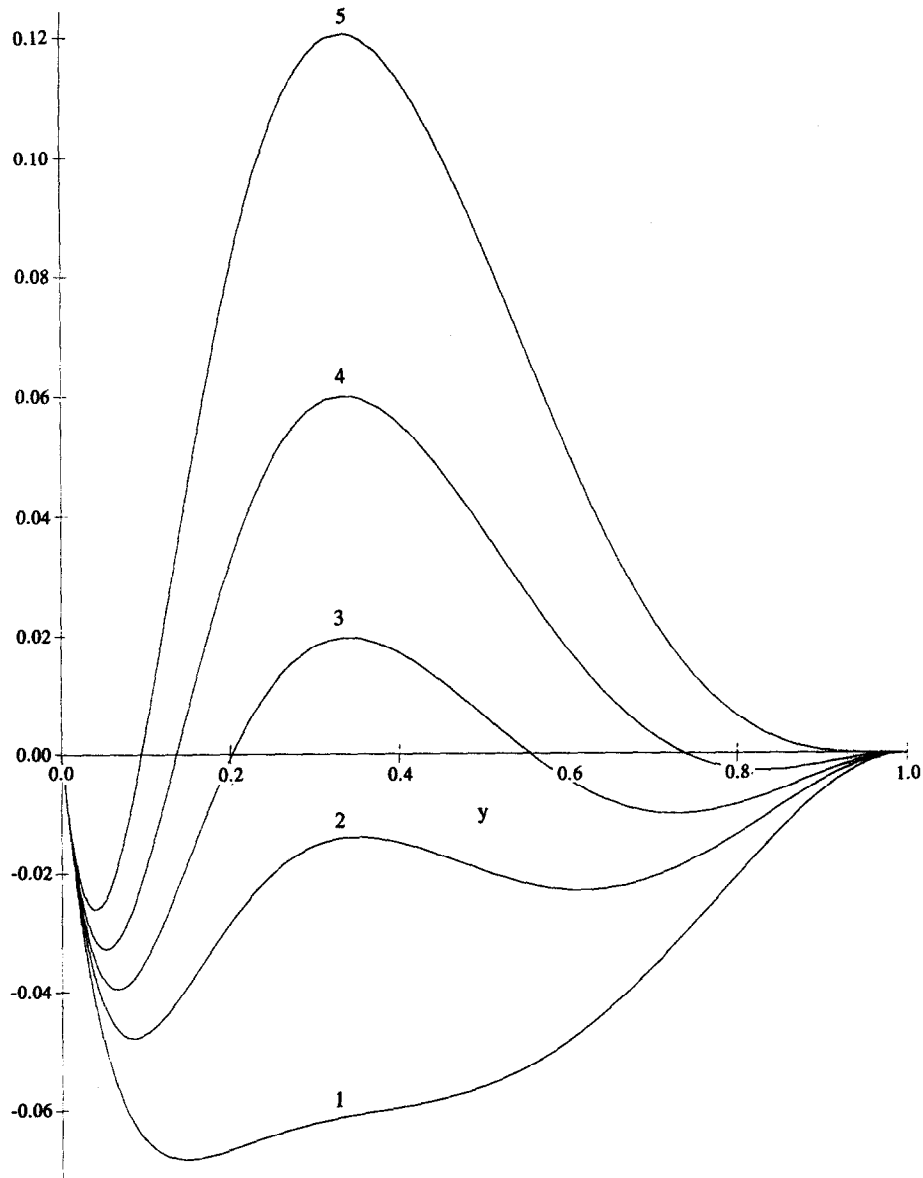


Fig. 3. Radial part of the streamfunction $\Psi/\sin 2\theta$ vs relative radial coordinate $y = (r-1)/(R-1)$ at $R = 2.5$: (1) $k = 6000$, (2) $k = 8333$, (3) $k = 10000$, (4) $k = 12000$, (5) $k = 15000$.

effects we have to carry out the numerical solution of the fully non-linear equations.

4. NUMERICAL STUDY OF FINITE-AMPLITUDE VIBRATIONAL FLOWS

A finite difference method was used for studying the non-linear behavior at arbitrary values of the parameters. The results of calculations are presented in

Figs. 6–8. The calculations were carried out at fixed value of the Prandtl number: $Pr = 1$.

The non-linear dynamic of the flow is determined by the parameters Gv and Sc separately. We choose two governing parameters Gv and ratio $k = Gv/Sc$ for the results description. In Fig. 6 the dependencies of the extremal values of the streamfunction on the vibrational Grashof number are presented for two different values of the parameter k . The curves 1 and

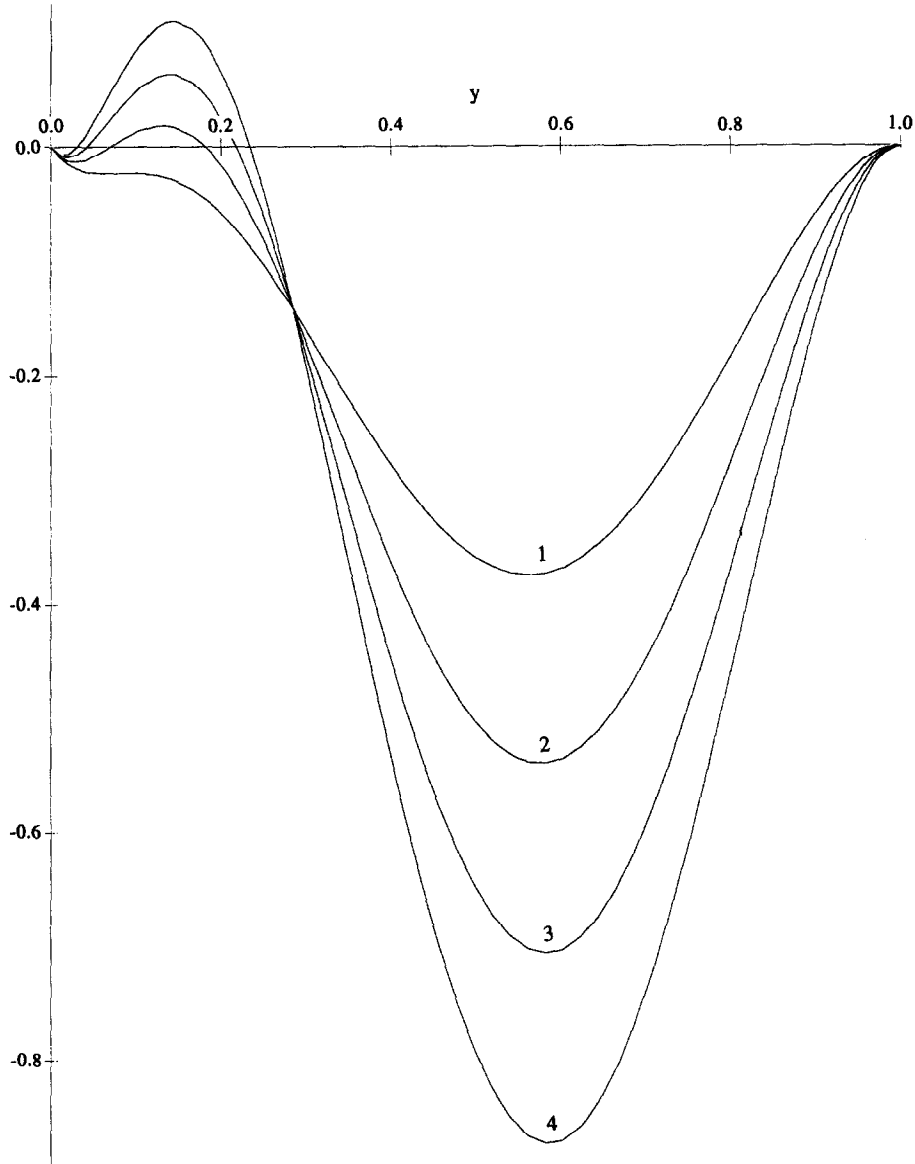


Fig. 4. Radial part of the streamfunction $\Psi/\sin 2\theta$ vs relative radial coordinate $y = (r-1)/(R-1)$ at $R = 2.1$: (1) $k = 50\,000$, (2) $k = 80\,000$, (3) $k = 100\,000$, (4) $k = 150\,000$.

2 correspond to $k = 10\,000$ and 8333 . As one can see at $k = 10\,000$ (curve 1) and small values of Gv the flow intensity slowly increases with the increase of the vibrational Grashof number. At $Gv \approx 2700$ a sharp increase of the flow intensity takes place.

In Fig. 7(a)–(d) the streamlines of the time-averaged steady flows obtained by numerical simulation at $k = 10\,000$ and four different values of Gv are presented. As one can see, at small values of Gv the flow structure is the same as the one obtained by analytical calculations under the restriction of creeping flow (Fig. 7a). This is a three-floor flow structure. The three

vortices are the Schlichting one placed near the inner sphere and the two thermovibrational vortices of different directions placed in the middle of the layer and near the outer sphere (as it was mentioned earlier there is one more Schlichting vortex near the outer sphere, but its intensity and size are so small that it cannot be seen in the picture being described in the unique scale). When the vibrational Grashof number increases, the two vortices of the same directions placed initially near the rigid surfaces join and replace the vortex of the opposite direction initially placed between them into the equatorial area (Fig. 7b). In

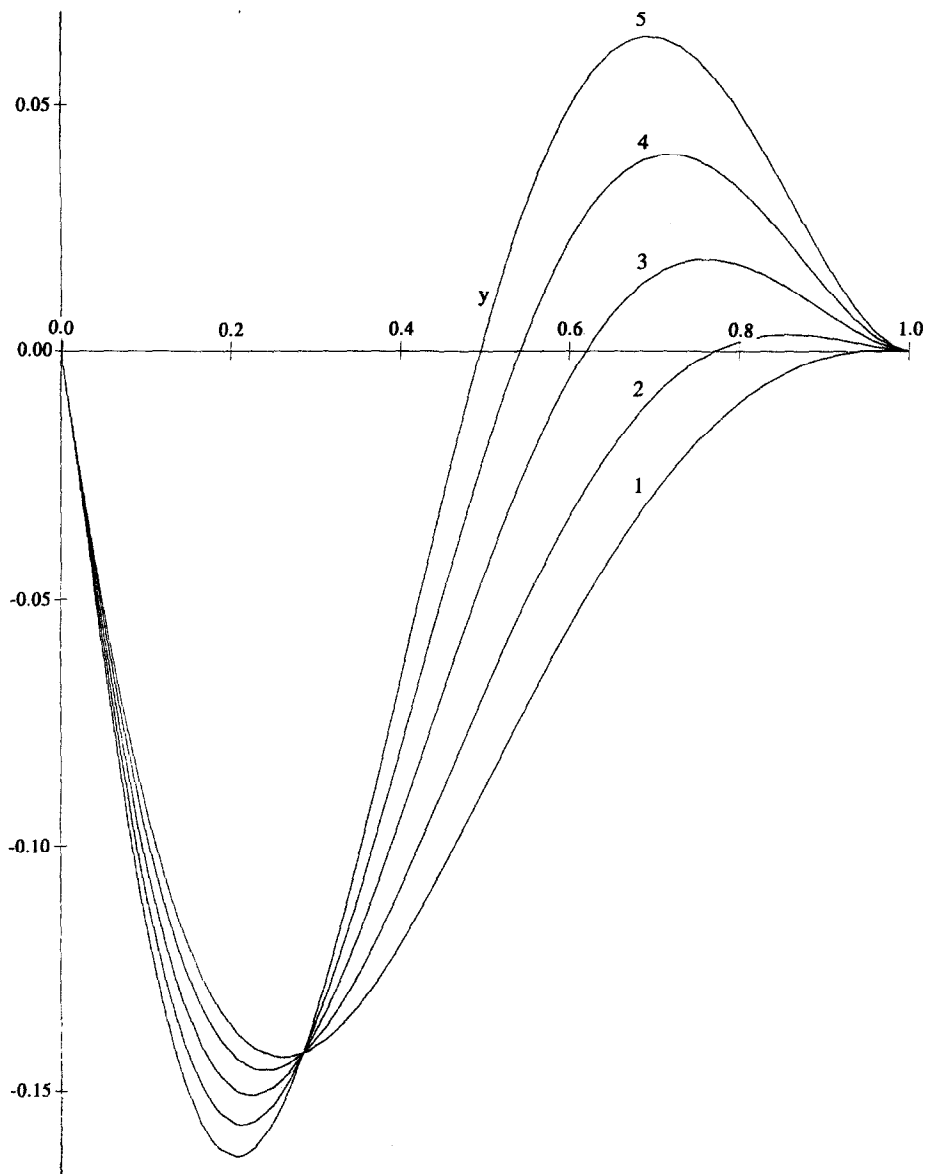


Fig. 5. Radial part of the streamfunction $\Psi/\sin 2\theta$ vs relative radial coordinate $y = (r-1)/(R-1)$ at $R = 2.1$: (1) $k = -6000$, (2) $k = -10\,000$, (3) $k = -15\,000$, (4) $k = -20\,000$, (5) $k = -25\,000$.

the vicinity of $Gv = 2700$ the transition from this flow structure to the one where the multi-vortex flow structure in azimuthal direction is clearly displaced (Fig. 7c) takes place. This transition in the flow structure is accompanied by a sharp increase of the extremal value of the streamfunction for the main vortex (Fig. 6, curve 1). With further increase of Gv , a continuous growth of the equatorial vortex size and intensity takes place so that at $Gv = 3500$ the polar and equatorial vortex intensities and sizes are actually the same (Fig. 7d).

Hysteresis phenomena were found to take place in the situation considered herein. As one can see from

Fig. 6, curve 1, the lowering of the vibrational Grashof number from $Gv = 4000$ up to $Gv \approx 2600$ leads to a slow decrease of the flow intensity and only at $Gv \approx 2600$ does the sharp decrease of the flow intensity take place. Thus, we observe the non-linear behavior typical for the perfect bifurcation. In such case one could expect the existence of the solutions branch corresponding to another preferable direction of circulation (strictly speaking even two branches should exist; one of which corresponds to the stable solutions and the other to the unstable ones). Actually, our calculations have shown the existence of the discussed branches. The branch of the stable solutions

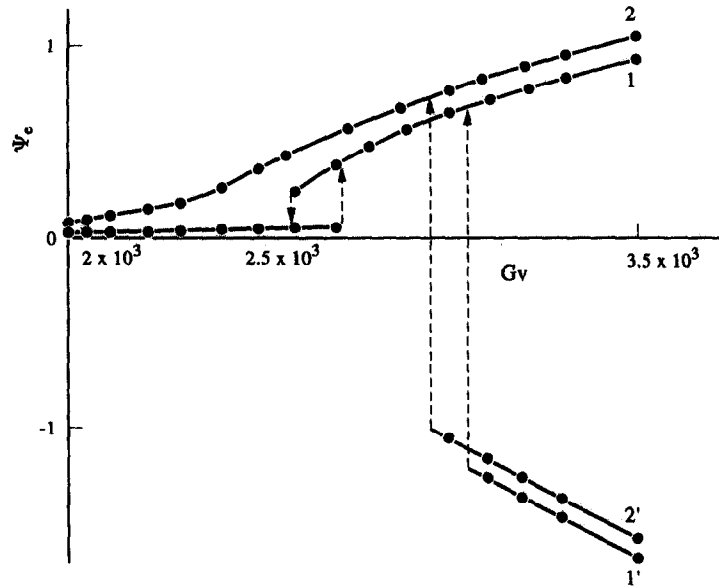


Fig. 6. Extremal values of the streamfunction vs vibrational Grashof number at $R = 2.5$: (1) and (1') $k = 10\,000$; (2) and (2') $k = 8333$.

is described in Fig. 6 (curve 1) and the flow structure is shown in Fig. 7e.

Similar phenomena are observed at $k = 8333$; but in that case the behavior is simpler. Then, at small values of the vibrational Grashof number, the flow structure corresponds to the one-vortex main flow and two weaker vortices of the same direction in the interior (Fig. 8). With the increase of the vibrational Grashof number, the two weak vortices combine into only one vortex. With further growth of the vibrational Grashof number the flow structure in the considered quarter of the sphere does not remain one-cellular, an additional weak vortex of the opposite direction appears near the equatorial plane. As in the case of $k = 10\,000$, the further growth of Gv leads to intensify this vortex so that at $Gv = 3500$ the two vortices are actually of the same intensity and size.

5. DISCUSSION

Thus, the high-frequency oscillations of a heated (or cooled) solid body immersed in a liquid induce time-averaged flow in that liquid due to two different mechanisms. The first of these mechanisms (the Schlichting one) acts even in the uniform fluid of constant density. In this case the pulsating flow in the thin viscous skin-layer near the vibrating body surface is of the vortex nature and, due to non-linear interaction, leads to time-averaged flow, which the vortex is as well. The second mechanism is a thermovibrational convective mechanism of a new type discovered in ref. [4]. This thermovibrational convective effect is linear with respect to small Boussinesq parameter $\beta\Theta$,

whereas the conventional thermovibrational convective effect [3] is of the second order with respect to $\beta\Theta$. As it is shown in ref. [4], the study of thermovibrational flows in the case (considered herein) of non-uniform vibrations should be performed taking into account the effect of the first order related to the spatial non-uniformity of isothermal pulsating velocity field. The calculations carried out in the present paper on the base of a new approach developed in ref. [4] display the particular features of the above-mentioned phenomena.

We have to point out that significant differences exist between the problem considered herein when an oscillating sphere placed in a fixed envelope (i.e. when the different parts of the boundary move in accordance with different laws), and the situation when the inner sphere and envelope oscillate in accordance with the same law.

In the latter case the isothermal pulsating velocity field is zero in the proper reference frame connected with the oscillating sphere; hence, contrary to the case considered herein, thermovibrational convective effect of the first order (with respect to small Boussinesq parameter $\beta\Theta$) is identically absent as well as isothermal vibrational Schlichting flow. Only the conventional thermovibrational convective effect (of the second order) takes place. Hence in that case, the conventional equations for the thermovibrational convection with the non-slip conditions for the time-averaged velocity on the rigid boundaries can be used.

This leads to a quite different resulting flow structure, namely (a) the flow structure becomes independent of the temperature difference sign between

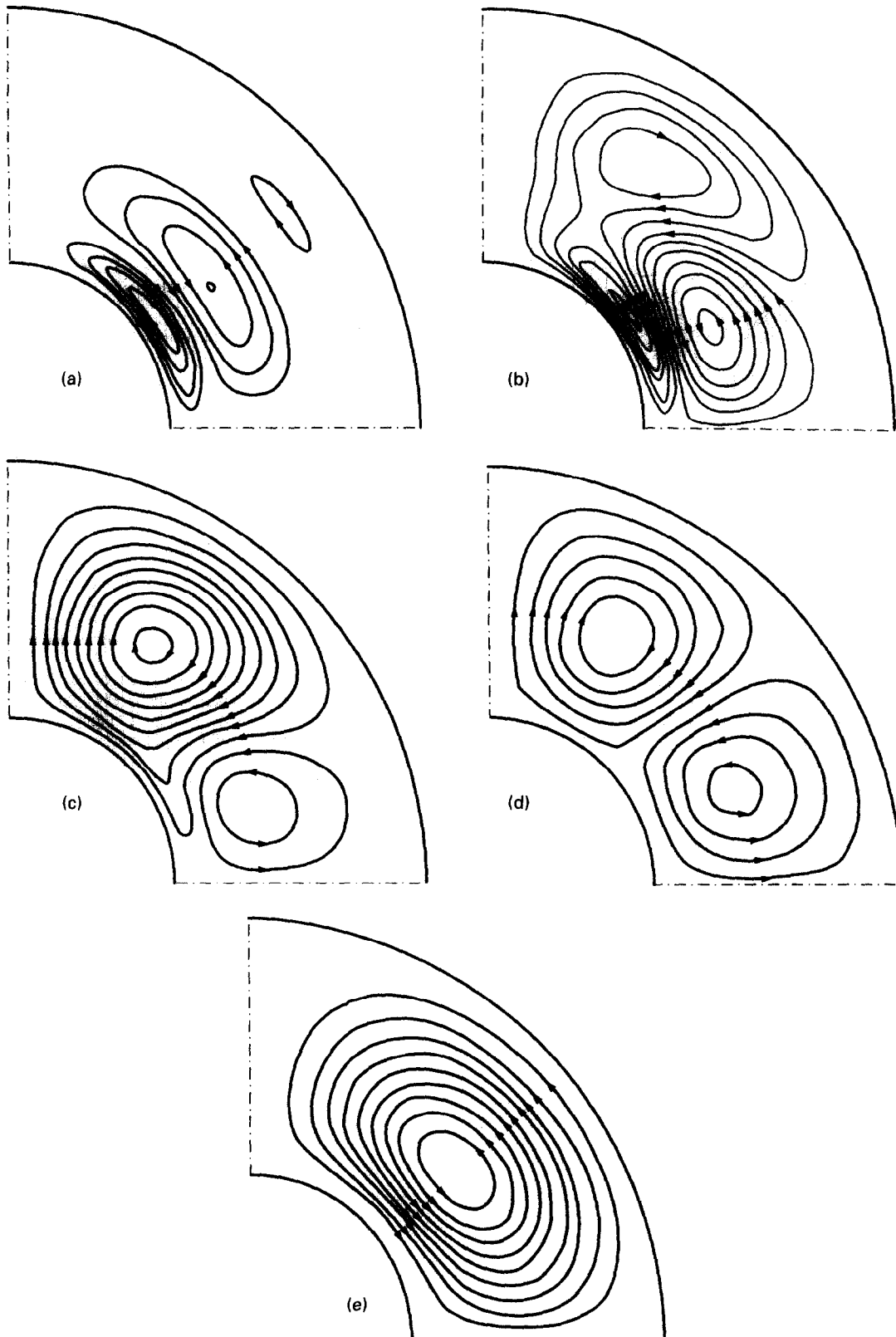


Fig. 7. Streamlines of the stationary flows at $R = 2.5$, $k = 10000$: (a) $Gv = 2000$, (b) $Gv = 2300$, (c) $Gv = 2600$, (d) $Gv = 3500$, (e) $Gv = 3500$ (1').

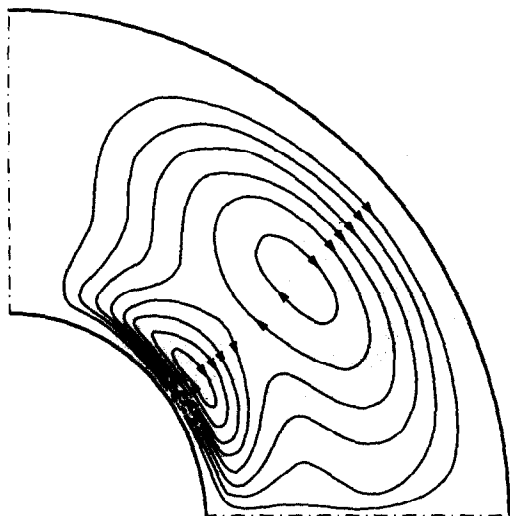


Fig. 8. Streamlines of the stationary flows at $R = 2.5$, $k = 8333$, $Gv = 1000$.

the inner sphere and envelope and (b) the absence of the Schlichting flow leads to the simplification of the resulting flow structure.

6. CONCLUSIONS

The time-averaged flows induced by the oscillations of a heated (or cooled) solid sphere immersed in a liquid have been investigated on the basis of new generalized equations of thermovibrational convection in non-uniform fluids. The two cases of infinite surrounding liquid and liquid placed into the spherical

rigid envelope are considered. The interaction of thermovibrational flows and the Schlichting flows has been elucidated.

Analytical investigation performed for small values of the governing parameters Sc and Gv , under the restriction of creeping flows, showed that the vibrational flow essentially depends on the layer thickness, and in the case of small thicknesses it can be rather complicated. At fixed thickness of the layer the creeping flow structure is defined by only one parameter which is the ratio of the vibrational Grashof number and the Schlichting parameter ($b \approx Gv/Sc$).

At larger values of the parameters Sc and Gv , the structure of vibrational flows depends on these two parameters, separately. The evolution of the flow with the increase of two parameters has been investigated by a finite difference method.

Acknowledgement—The present research was made possible by grant MF 5000 from the International Science Foundation.

REFERENCES

1. G. Schlichting, *Grenzschicht-Theorie*. Braun, Karlsruhe (1965).
2. G. Z. Gershuni and E. M. Zhukhovitsky, Vibration-induced thermal convection in weightlessness, *Fluid Mech. Sov. Res.* **15**, 63 (1986).
3. S. M. Zenkovskaya and I. B. Simonenko, On the high frequency vibration influence on the onset of convection, *Izv. AN SSSR Mekh. Zhidk. Gaza* **5**, 51 (1966).
4. D. V. Lyubimov, Thermovibrational flows in a fluid with a free surface *Micrograv. Q.* **4**(2), 107 (1994).
5. Physical Acoustics. Principles and methods. In *Properties of Polymers and Nonlinear Acoustics* (Edited by W. P. Mason), Vol. 2, Part B. Academic Press, New York (1965).